

A Hybrid Piezoelectric Structure for Wearable Nanogenerators

Minbaek Lee, Chih-Yen Chen, Sihong Wang, Seung Nam Cha, Yong Jun Park, Jong Min Kim, Li-Jen Chou, and Zhong Lin Wang*

The concept of human-motion-based energy harvesting has huge technological interest in accordance with the growing popularity of portable smart electronics. It is becoming more feasible, due to advanced research in nanoelectronics, to operate at an extremely low power consumption, so that energy scavenged from the environment may be sufficient to meet the working mode.^[1–3] Solar and thermal energies are the most-common and feasible sources of energy to be scavenged from our surroundings. However, these types of energy are time and location dependent. Especially for personal electronics, mechanical energy is the most-likely reliable and independent energy source, since human activities are based mostly on mechanical movement, regardless of environment. Harvesting energy from body motion or human activity has a strong potential, which can untie modern personal life from the messy connections of wires for electric power supply. According to such a concept, nanowire-based nanogenerators (NGs) built on textile fibers or solid substrates have been demonstrated for the harvesting of mechanical energy produced by the friction-motion of two fibers or ultrasonic waves.^[4,5] Until now, for scavenging of energy from mechanical movement, especially human activity, it has been important to explore wearable and sustainable technologies that work at low frequencies and at various amounts/directions of deformation, and that are based on flexible and durable materials.

Herein, we present a simple but practical and durable approach that converts low-frequency (<1 Hz) mechanical activity into electricity using hybrid piezoelectric materials. Our device was composed of zinc oxide nanowires (NWs) and poly(vinylidene fluoride) (PVDF) polymer around a conducting fiber, which is a unique hybridization of two piezoelectric materials. The zinc oxide NWs served as a piezoelectric-potential

generator and as an additive to enhance the surface-contact area, which guided the formation of a uniform layer of piezoelectric polymer (i.e., PVDF) around the fiber during the dip-coating process. The PVDF polymer also plays multiple roles, such as in the piezoelectric ensemble with the ZnO NWs and as a protective material for high durability under deformation. By elongating or bending the hybrid fiber, mechanical energy is converted into electricity owing to constructive piezoelectric-potential generation from the two components (i.e., PVDF and ZnO NWs). This work may lead to an innovative way to a fiber-type wearable technology that harvests energy from the physical activity of living creatures.

To explore the feasibility of hybridizing two different piezoelectric materials, such as ZnO NWs and PVDF, hybrid layers were initially fabricated on plane-type substrates. Flexible Kapton (model 500HN, DuPont Inc.) was utilized as the substrate for the plane-type devices in our experiment. The hybridized structure is shown in **Figure 1**. It was a laminated structure (**Figure 1a**), composed of a top Au/Cr electrode (50 nm/10 nm), a ZnO-NW array infiltrated with PVDF (100 μm), a Au/Cr counterelectrode (50 nm/10 nm), Kapton (125 μm) and a supporting polystyrene (PS) substrate (500 μm). The supporting PS substrates were attached to the plane-shaped NGs for the driving of identical strains throughout the active piezoelectric layer.^[6,7] **Figure 1b** and its inset are scanning-electron-microscopy (SEM) images with low and high magnifications, respectively, showing the ZnO-NW arrays synthesized on the Au/Cr/Kapton substrate by a hydrothermal method.^[8–10] It is well known that the physical properties and crystalline structure of ZnO NWs depend on the various growth methods.^[10] Here, a hydrothermal process with a Au seed layer was chosen for the NG fabrication because of future feasibility for wearable electronics. The ZnO-NW arrays were expected to serve not only as a piezoelectric material, but also as an additive to enhance the stability of the PVDF film by increasing the contact surface area (**Figure S1**, Supporting Information). To infiltrate the piezoelectric polymer into the spaces around the NWs, PVDF polymer dissolved in acetone and *N,N*-dimethylformamide (DMF) solvents was spin-cast at a speed of 1000 rpm for ≈ 60 s, and the solvents were completely dried off under ambient conditions. **Figure 1c** and its inset show the top surface of the device after coating of a PVDF layer on a ZnO-NW-grown substrate at low and high magnifications, respectively. The polymer layer covered the ZnO-NW arrays fully and maintained a relatively superior stability, compared with ones without ZnO-NW arrays. This implies that NW arrays can improve the stability of a PVDF film virtually on any substrate. Lastly, a second electrode was deposited on the top of the PVDF surface via a thermal-evaporation

Dr. M. Lee,^[+] C.-Y. Chen,^[+] S. Wang,
Prof. Z. L. Wang
School of Materials Science and Engineering
Georgia Institute of Technology
Atlanta, GA 30332, USA
E-mail: zlwang@gatech.edu

Dr. C.-Y. Chen, Prof. L.-J. Chou
Department of Materials Science and Engineering
National Tsing-Hua University
Hsinchu, 30013, Taiwan

Drs. S. N. Cha, Y. J. Park, J. M. Kim
Frontier Research Lab, Samsung Advanced Institute of Technology
Samsung Electronics
Gyeonggi-Do 446-712, Korea

[+] These authors contributed equally to this work.



DOI: 10.1002/adma.201200150

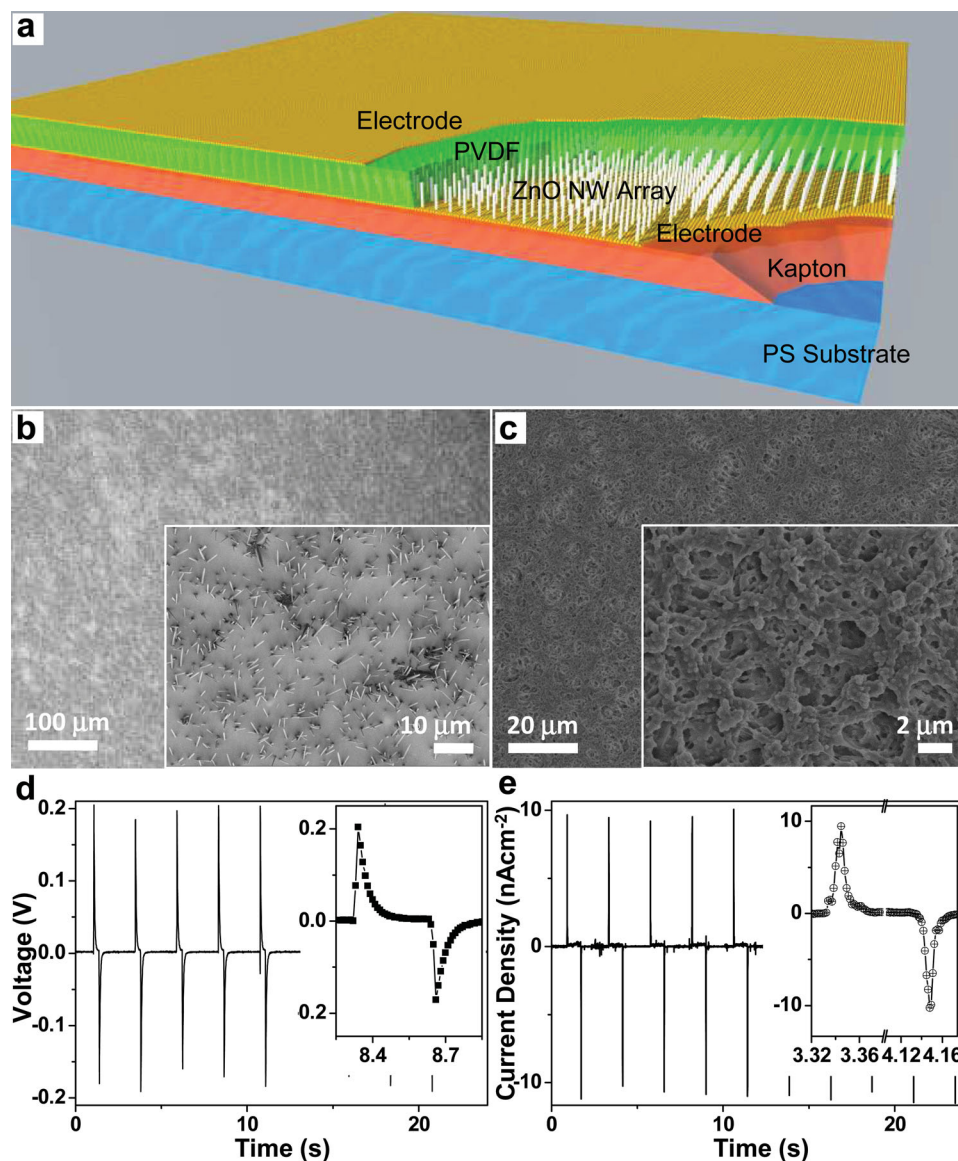


Figure 1. Schematic diagram and SEM images of a plane-shaped hybrid nanogenerator. a) Schematic 3D diagram depicting the structure of the hybrid device in plane-shape. The ZnO NWs and the PVDF polymer were placed in between two Au electrodes and played the key role for mechanical-energy conversion. The bottom PS plate served as a supporting substrate to deliver a uniform mechanical stress on the active layer. b) An SEM image of a ZnO-NW array grown on the Au film/Kapton substrate. The inset shows a magnified SEM image. c) An SEM image of the top surface of the PVDF layer on the ZnO NWs grown on the Au/Kapton substrate. The inset shows a magnified SEM image. d) Electrical characteristics of plane-shaped nanogenerators based on the hybrid piezoelectric material (i.e., PVDF and ZnO-NW array). Open-circuit output voltage of a hybrid nanogenerator. e) Closed-circuit output current density of a hybrid nanogenerator.

method to complete the hybrid, plane-shaped NG (see also Figure 1a).

Utilizing the hybrid, plane-shaped NG, we contemplated the power output of the hybrid piezoelectric structure. A plane-type hybrid NG was loaded on a stage, on which a linearly moving motor was installed to apply a strain to the NG at a relatively low frequency (<1 Hz). Figure 1d and 1e show the open-circuit voltage and the closed-circuit current output from our hybrid NG. The peak values of the voltage, current and power density were found to be 0.2 V, 10 nA cm⁻² and 2 μW cm⁻³, respectively. In the power-density calculation, the active volume of the

piezoelectric material (i.e. the fraction of ZnO NWs and PVDF) in our fiber device was solely considered. Throughout all of the measurements, the mechanical motion was applied to the NG over a frequency range of ≈ 0.25 –1 Hz, since human activities are mainly in the low-frequency regime. As a comparison, the electrical output was also investigated for a PVDF-thin-film-based generator without the presence of the ZnO-NW array (Figure S2, Supporting Information). The peak values of the voltage, current and power density from the control device were found to be 0.18 V, 5 nA cm⁻² and 1 μW cm⁻³, respectively. A plausible explanation is that the uniquely coupled properties of

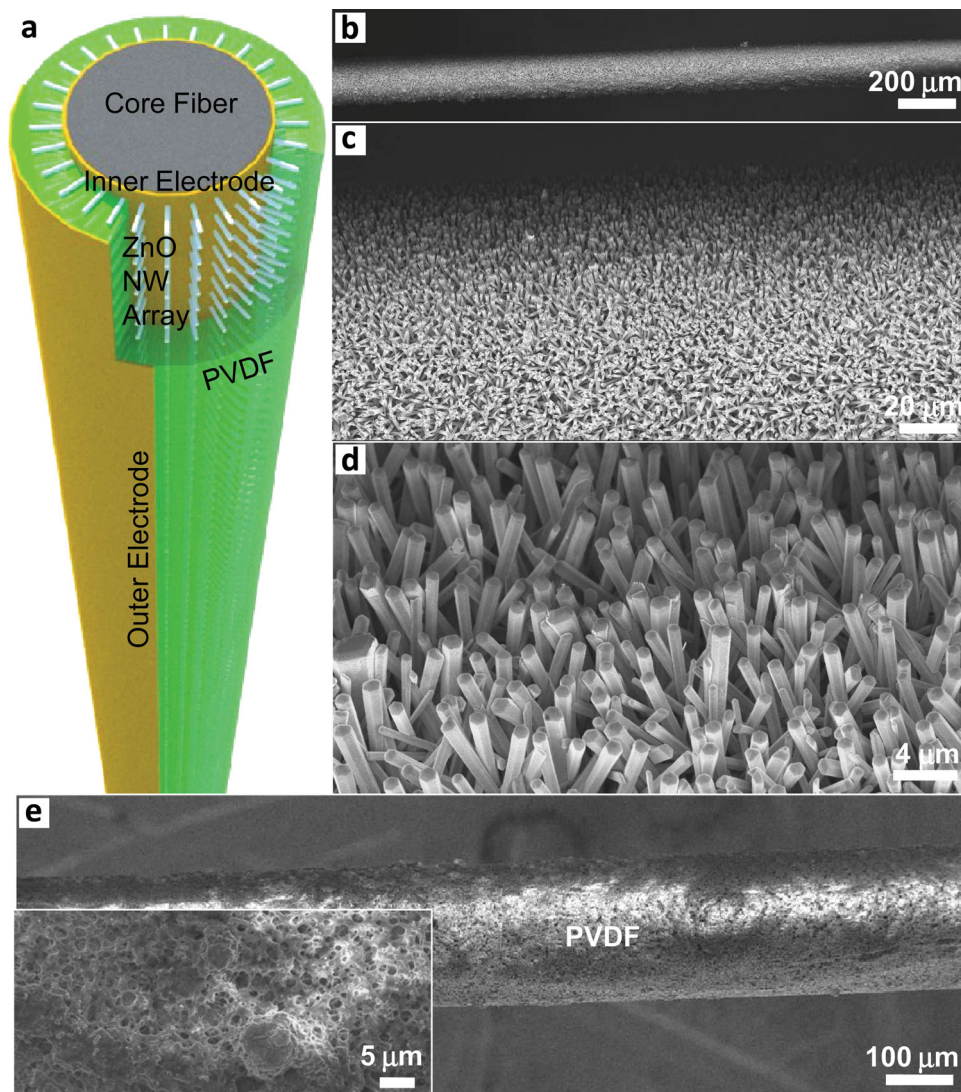


Figure 2. Schematic diagram and SEM images of the hybrid-fiber device. a) Schematic 3D diagram depicting the structure of a hybrid-fiber nanogenerator. The ZnO NWs and the PVDF polymer were placed in between two Au electrodes and played the key role for mechanical-energy conversion. b) SEM image of the ZnO-NW array grown on a Au-coated fiber. c–d) Magnified SEM images. e) SEM image of the surface of a PVDF layer on the ZnO-NW grown fiber. The inset shows a magnified SEM image of the surface of the PVDF layer.

the ZnO NWs affect the piezoelectric coefficient of the hybrid piezoelectric structure. PVDF is known to have a negative piezoelectric coefficient, d_{33} , while ZnO NWs have a positive value. Because of the inherent piezoelectricity of the ZnO NWs, a poling process is unnecessary. Thus, PVDF can be safely poled along any desired direction. This allows us to align the dipoles, which leads to a positive output of our hybrid device. Aside from the aligned piezoelectricity of the hybrid structure, during the poling process of the PVDF polymer, the ZnO-NW arrays may also assist as semiconducting electrodes, resulting in a superior piezoelectric coefficient of the PVDF polymer. This result indicates that our hybrid approach can enhance the contact surface area of two different piezoelectric materials and also affect the electrical-power output and stability of a PVDF-polymer layer on the substrate.

In accordance with the experiments with the plane-shaped NGs, ZnO-NW arrays were also utilized in the fabrication of hybrid-fiber NGs as piezoelectric materials and as an additive for the enhancement of the surface area. In this case, the ZnO NWs served as pillars to hold a PVDF solution for the following dip-coating process, so that the hybrid fibers could have a uniform outermost surface with the piezoelectric polymer. **Figure 2a** shows a schematic diagram depicting the structure of our hybrid-fiber generator. Firstly, Au film was coated on a bare fiber, playing the roles of an inner electrode and a seed layer for the following growth of the NWs on the fiber. A hydrothermal process^[8–10] was conducted for the growth of the ZnO NWs, which covered the fiber uniformly with a radial alignment (Figure 2b–d). During the PVDF dip-coating process, NWs on the fiber successfully assisted the

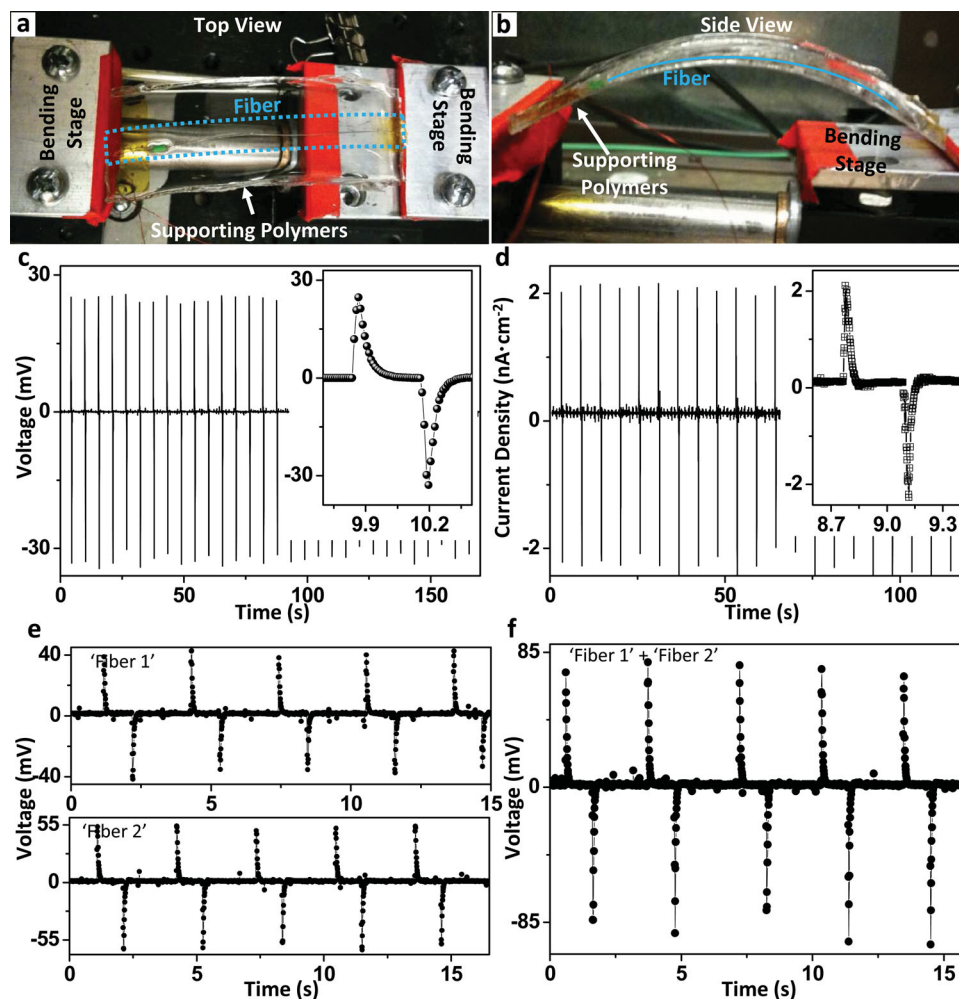


Figure 3. Optical images and electrical characteristics of hybrid-fiber nanogenerators. a) Top-view of a hybrid-fiber device loaded on the bending stage. The hybrid-fiber device was attached on a plane PS substrate and covered with PDMS to experience a uniform stress during the measurements. b) Side-view of a hybrid-fiber device loaded on the bending stage. c) Open-circuit output voltage of a fiber device under a strain of $\sim 0.1\%$. d) Closed-circuit output current density of a fiber device under a strain of $\sim 0.1\%$. e) Open-circuit voltage outputs of two different fiber devices under a strain of $\sim 0.1\%$. The hybrid devices labeled 'Fiber 1' and 'Fiber 2' reached ~ 40 mV (top) and ~ 55 mV (bottom), respectively. f) Superimposed open-circuit voltage output of the two fiber devices connected in series under a strain of $\sim 0.1\%$ and at a strain rate of $\sim 2.3\% \text{ s}^{-1}$.

formation of a PVDF layer, acting like micropillars (Figure 2e and inset). An additional Au film was deposited on half of the outermost surface and served as the other electrode for the poling of PVDF and the energy-scavenging process later on. The applied electric field reached 100 kV mm^{-1} during the poling process.^[11–13] Since our hybrid fiber was composed of two different piezoelectric materials, aligning of their dipoles was crucial to hybridize them positively. In the hybrid-fiber fabrication, the PVDF was poled along the direction of the *c*-axis of the ZnO-NW arrays to align the piezoelectric dipoles in the active piezoelectric layer.

The electrical measurement of the output power was conducted for our hybrid-fiber generator (Figure 3). In the measurements, the covering polymer and supporting substrate were adjusted to the fiber generator to apply an identical strain along the whole device.^[14,15] This consisted of a PS substrate and a PDMS covering layer. A PS plastic plate served

as the bottom supporter and the PMDS layer covered and held the device to deliver an identical strain under a certain external stress. Figure 3a and 3b show optical images of our fiber device embedded in PDMS polymer on a PS substrate. The thicknesses of the PS substrate, the PMDS layer and the fiber device were 1 mm, 5 mm and 0.2 mm, respectively. The embedded device was loaded on the bending stage to receive an external stress. The fiber generator was bent along with the supporting polymer; thus, the whole fiber was assumed to experience an identical strain (see also Figure S3, Supporting Information). Under $\sim 0.1\%$ strain, our hybrid-fiber generator reached an open-circuit voltage (Figure 3c) and a closed-circuit current density (Figure 3d) of 32 mV and 2.1 nAcm^2 , respectively. Compared with the output power of the first fiber NG, with ZnO NWs and a vacant volume area in between the NW forest,^[4] our hybrid-fiber NG exhibits an enhanced performance owing to the volume-effective hybridization of the

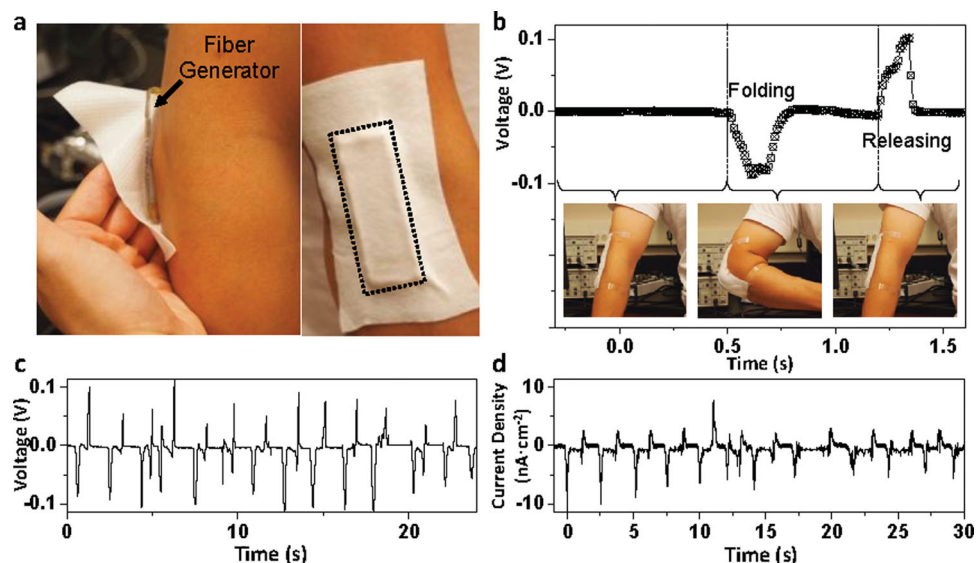


Figure 4. Electrical measurements of our hybrid-fiber nanogenerator attached on a human arm. a) Optical images of the hybrid-fiber device attached on an elbow. The hybrid-fiber device was attached on a plane PS substrate and covered with PDMS to experience uniform stress during the measurements. The device in the PDMS/PS supporting polymers was attached on the elbow. b) Open-circuit voltage output of a fiber device depending on the folding and releasing of the elbow. A voltage output appeared on the event of the folding and releasing action of the elbow. The elbow was held for an angle of $\sim 90^\circ$. c) Open-circuit voltage outputs of a fiber device during multiple folding-releasing events of the elbow. d) Closed-circuit current-density output of a fiber device during multiple folding-releasing events of the elbow.

polymeric piezoelectric material (i.e., PVDF) instead of the vacant volume area. For practical application and to rule out noise caused by other effects,^[16] a superposition of the generated outputs from the fiber devices should be investigated. It is also subject to compatibility with other microelectronic devices for future use, such as rectifying circuits, wireless transmitters, laser-emitting diodes and other sensors that require a practical amount of voltage output.^[17] To avoid any variation in the applied strain from one fiber device to the other, multiple fiber NGs were placed in the same supporting polymer (Figure S4, Supporting Information); thus, they could experience an almost-identical strain during the superposition experiment. Two adjacent fiber devices were selected for the experiment, since they were expected to be under the same conditions of strain (0.1%) and strain rate ($2.3\% \text{ s}^{-1}$). The selected two fibers showed open-circuit voltage outputs of $\sim 40 \text{ mV}$ and $\sim 55 \text{ mV}$, respectively (Figure 3e). Afterwards, the fibers were connected in series and the electrical measurement was performed likewise. The output voltage was found to be $\sim 85 \text{ mV}$ (Figure 3f), which implies the potential of the integration of fiber generators for future applications. The loss of voltage output can be explained by the leakage of electric charge through the devices and through the resistive wiring of the two fiber devices.

Since our device was aimed towards wearable electronics capable of scavenging energy from human activity, it was attached onto a human arm to evaluate its performance depending on human movement. The PS/PDMS protecting polymers were also adjusted in this demonstration to prevent any direct contact of the device with human skin, which could cause undesired electrical noise. The fiber device embedded

in the polymer was firmly attached on an elbow, as shown in Figure 4a, so that it could experience enough strain from the folding and releasing actions of the arm. In accordance with the moving action of the human arm, a single fiber device exhibited voltage and current-density outputs of $\sim 0.1 \text{ V}$ and 10 nA cm^{-2} , respectively (Figure 4b–d; also see a video clip Supporting Information). When the active volume of the piezoelectric materials (i.e., the fraction of ZnO NWs and PVDF) in our fiber device was solely considered, the output power density was estimated to be $\sim 16 \mu\text{W cm}^{-3}$. The novel structure of our hybrid fiber has much room to be improved in the future simply by replacing the piezoelectric materials with high-performance polymers^[18] and controlling the structure of the ZnO.^[19] This should inspire the research field of wearable electronics that harvest electrical energy from the mechanical activity of living creatures.

In summary, we have demonstrated hybrid-fiber generators that show a high performance and feasibility as the power source for wearable electronics. The hybrid-fiber NGs employed a unique piezoelectric layer, which comprised ZnO NWs and a PVDF infiltrating polymer. The NW array served not only as the piezoelectric material, but also assisted the formation of PVDF on the outermost surface of the device. By attaching our hybrid-fiber device, with a length of $\sim 2 \text{ cm}$, on the human arm, the output voltage, current density and power density reached 0.1 V , 10 nA cm^{-2} and $16 \mu\text{W cm}^{-3}$, respectively, under folding-releasing of an elbow for $\sim 90^\circ$. This indicates that our fiber NG suggests a highly promising structure as an energy harvester that converts low-frequency mechanical movements of human/animal activity into electricity. Our innovative approach may also inspire the research area for future wearable electronics.

Experimental Section

Fabrication of the Nanogenerators: Flexible plane- and fiber-type substrates were utilized as substrates for hybrid-NG fabrication. Firstly, the substrate was rinsed with acetone, methanol and deionized (DI) water, in series. Conducting Au (50 nm)/Cr (10 nm) film was deposited via a thermal-evaporation method as the seed layer for ZnO-NW growth, and as an electrode. In the case of the fiber-type NGs, the evaporation process was conducted twice (i.e., on one side and then the other) to coat a Au film on the surface of the fibers. Afterwards, a hydrothermal method was utilized for the growth of NW arrays on two kinds of substrate.^[8] In this process, a part of the Au seed layer remained for the later electric-contact pad by screening a nutrient solution. The nutrient solution was produced with DI water, hexamethylenetetramine (HMTA) and zinc nitrate hexahydrate ($\text{ZnNO}_3 \cdot 6(\text{H}_2\text{O})$), resulting in an $\sim 10 \times 10^{-3}$ M solution. During the growth, the plane-type substrates were placed on the top of the solution, upside downward, while the fiber-type ones were dipped and held in the mid-area of the solution to avoid the bottom area of the solution. They were heated up to 85 °C for ~ 16 h in an isothermal oven to grow the NW arrays. The NW-grown substrates were rinsed with DI water and gently blown with nitrogen gas. Then, PVDF (1.5 g of PVDF in 20 mL of acetone/DMF solvent with the volume ratio of 6:4) was spin-coated on the plane-type substrate at 1000 rpm for ~ 60 s, or dip-coated on the fiber-type substrates. In the case of the dip-coating process, the whole fiber devices were thoroughly dipped in the PVDF solution and pulled out slowly at a speed of ~ 5 mm s^{-1} . The surfaces of our fibers were decorated with dense and radially aligned ZnO NWs, which served as holding poles for the PVDF solution during the dip-coating and drying processes. Afterwards, another Au (50 nm)/Cr (10 nm) layer was deposited on the top of the PVDF polymer via a thermal-evaporation method, for the fabrication of the other electrode.

Electrical Measurements: All of the electrical characterizations of the NGs were conducted after connecting the two Au film layers as electrodes in both the plane-type and fiber-type devices. A home-made bending stage (see Figure 3a and 3b) served to apply a periodic deformation to the NGs at the desired frequency (< 50 Hz) and speed. The short-circuit current and the open-circuit voltage were measured via current and voltage preamplifiers (Stanford Research SR570 and SR560), respectively.

Supporting Information

Supporting Information is available from the Wiley Online Library or from the author.

Acknowledgements

The research was supported by Samsung, DARPA (HR0011-09-C-0142, Program manager, Dr. Daniel Wattendorf) and the US Department of Energy, the Office of Basic Energy Sciences, the Division of Materials Sciences and Engineering under Award DE-FG02-07ER46394.

Received: January 11, 2012

Published online: March 7, 2012

- [1] M. S. Dresselhaus, I. L. Thomas, *Nature* **2001**, 414, 332.
- [2] Z. L. Wang, *Sci. Am.* **2008**, 298, 82.
- [3] Z. L. Wang, *Adv. Funct. Mater.* **2008**, 18, 3553.
- [4] Y. Qin, X. D. Wang, Z. L. Wang, *Nature* **2008**, 451, 809.
- [5] X. D. Wang, J. H. Song, J. Liu, Z. L. Wang, *Science* **2007**, 316, 102.
- [6] R. S. Yang, Y. Qin, L. M. Dai, Z. L. Wang, *Nat. Nanotechnol.* **2009**, 4, 34.
- [7] J. H. Jung, M. Lee, J. I. Hong, Y. Ding, C.-Y. Chen, L. J. Chou, Z. L. Wang, *ACS Nano* **2011**, 5, 10041.
- [8] L. Vayssieres, *Adv. Mater.* **2003**, 15, 464.
- [9] Z. W. Pan, Z. R. Dai, Z. L. Wang, *Science* **2001**, 291, 1947.
- [10] S. Xu, Z. L. Wang, *Nano Res.* **2011**, 4, 1013.
- [11] A. M. Vinogradov, S. C. Schumacher, E. M. Rassi, *Int. J. Appl. Electromagn. Mech.* **2005**, 22, 39.
- [12] H. S. Nalwa, *Ferroelectric Polymers: Chemistry, Physics and Applications*, Marcel Dekker, Inc, New York **1995**, Part 1, Ch. 2, 3.
- [13] S. J. Kang, Y. J. Park, J. Sung, P. S. Jo, C. Park, K. J. Kim, B. O. Cho, *Appl. Phys. Lett.* **2008**, 92, 3.
- [14] Y. F. Hu, Y. Zhang, C. Xu, G. A. Zhu, Z. L. Wang, *Nano Lett.* **2010**, 10, 5025.
- [15] K. I. Park, S. Xu, Y. Liu, G. T. Hwang, S. J. L. Kang, Z. L. Wang, K. J. Lee, *Nano Lett.* **2010**, 10, 4939.
- [16] M. Lee, J. Bae, J. Lee, C. S. Lee, S. Hong, Z. L. Wang, *Energy Environ. Sci.* **2011**, 4, 3359.
- [17] G. A. Zhu, R. S. Yang, S. H. Wang, Z. L. Wang, *Nano Lett.* **2010**, 10, 3151.
- [18] K. Omote, H. Ohigashi, K. Koga, *J. Appl. Phys.* **1997**, 81, 2760.
- [19] Y. Hu, L. Lin, Y. Zhang, Z. L. Wang, *Adv. Mater.* **2012**, 24, 110.